

Assessment of Spatial Patterns and Drivers of Respiratory Health Risks Based on Air Pollution Spatiotemporal Data in Shenyang City, China

Zhenxing Li,¹ Yu Shi,² Peiying Li,¹ Xiaojuan Xing,³
Jingxue Xie,⁴ Tiemao Shi,^{5*} and Yaqi Chu

¹School of Architecture and Urban Planning, Shenyang Jianzhu University,
No. 25, Hunnan Middle Road, Hunnan District, Shenyang, Liaoning 110168, China

²School of Design and Art, Shenyang Jianzhu University,

No. 25, Hunnan Middle Road, Hunnan District, Shenyang, Liaoning 110168, China

³Beijing Institute of Surveying and Mapping, No. 60 Nanlishi Road, Xicheng District, Beijing 10045, China

⁴United Graduate School of Agricultural Science, Tokyo University of Agriculture and Technology,
Fuchu, Harumicho, 3 Chome-8-1, Tokyo 183-8538, Japan

⁵Institute of Space Planning and Design, Shenyang Jianzhu University,
No. 25, Hunnan Middle Road, Hunnan District, Shenyang, Liaoning 110168, China

⁶School of Architecture and Engineering, Shenyang University,
No. 25, No.21, Wanghua South Street, Dadong District, Shenyang, Liaoning 110003, China

(Received April 12, 2024; accepted June 18, 2024)

Keywords: respiratory health, geodetector, spatial pattern of risk, spatial environmental elements, interaction effects

Studying the spatial pattern distribution of respiratory health risks and the role of spatial environmental factors can improve our understanding of pathogenic mechanisms in the spatial environment. However, previous air quality index (AQI) sensor models lacked comprehensive air quality reflection, limiting risk prediction accuracy. In this study, we improved the AQI sensor model and combined it with population density data to establish a respiratory health risk exposure assessment model. Twenty-five spatial environmental variables were selected as potential factors. Pearson correlation analysis and a geodetector were used to assess the spatial risk patterns of respiratory diseases and determine the characteristics of the selected factors. The results indicated that (1) the health risk index showed autumn < summer < spring < winter ranking, with the health risk gradually decreasing from the center outwards. (2) The positive effect of the volume ratio, a spatial morphology factor, was the strongest, and the negative effect of the sky openness was the greatest. (3) The geodetector results showed significant spatial heterogeneity in the degree of effect of the spatial environmental factors on respiratory health risks. Moreover, the explanatory power of the interaction between any two factors (except the volume ratio) far exceeded that of a single factor.

*Corresponding author: e-mail: tiemaos@sjzu.edu.cn
<https://doi.org/10.18494/SAM5052>

1. Introduction

According to the World Health Organization (WHO), three of the ten leading causes of death worldwide are related to the respiratory system, and respiratory diseases have become a major threat to the health of the global population.⁽¹⁾ The respiratory system is an exogenous system of the human body. Air pollution has a direct effect on respiratory diseases. Although major atmospheric pollutants can cause various diseases in the human respiratory, circulatory, and other systems, they pose the greatest threat to the human respiratory system.⁽²⁾ China's rapid economic development has led to serious air pollution problems, resulting in more prominent respiratory health problems among Chinese residents.⁽³⁾

According to epidemiological studies, the occurrence of respiratory diseases is caused mainly by environmental exposure, and rapid urbanization and the overcrowding of the population can exacerbate the occurrence of acute and chronic respiratory diseases. There are many atmospheric pollutants, among which sulfur dioxide (SO₂), nitrogen oxides (NO_x), carbon monoxide (CO), ozone (O₃), and total suspended particulate matter (TSP) are the most threatening to human respiratory health.⁽⁴⁾ Air quality index (AQI) is now widely used in China as a method for calculating air quality. The method of calculating AQI involves comparing the concentration limits of various pollutants and calculating subindices, with the overall index determined by the maximum subindex of pollutants.⁽⁵⁾ The AQI calculation method neglects the cumulative and synergistic effects of various pollutants, leading to a blurred representation of individual pollutant information on an annual time scale and obscuring the overall pollution levels of different pollutants on a daily time scale.⁽⁶⁾ The latest WHO findings showed that low concentrations of air pollutants can still cause damage to the human respiratory system.⁽⁷⁾ However, at present, China still follows the previous classification standards for air pollutant concentrations. This may cause the public to misjudge the air quality and thus fail to take necessary protective measures. Accurate data for monitoring air pollution were the basis for improving environmental quality and developing protection strategies. The monitoring of air pollution in various Chinese cities was mainly based on fixed-point monitoring, a method that was insufficient to monitor the dynamics of the spatial distribution of air pollutants, although it could obtain monitoring data over a continuous period of time.⁽⁸⁾ The remote sensing monitoring method can utilize satellites, drones, or other remote sensing technologies to obtain air quality data on a large scale. This method can help to analyze the spatial and temporal patterns of air pollution, thus providing insight into the dynamics of air pollutant concentrations and their potential impact on health.

Li *et al.* introduced methods such as statistics and machine learning into the evaluation of air quality in order to solve the problem that the method of calculating AQI cannot fully reflect the real air quality, including index evaluation, principal component analysis, an analytic hierarchy process, artificial neural networks, fuzzy comprehensive evaluation, gray clustering, and set pair analysis, to improve AQI evaluation methods;^(9,10) their goal was to increase the accuracy and reliability of more effective assessments of air quality conditions. Despite some progress in improving AQI calculation methods, current research still faces unresolved issues. Although advanced models and methods have been employed to improve the accuracy and stability of the

AQI under complex meteorological conditions, especially during extreme weather events such as dust storms or typhoons, areas for improvement remain.⁽¹¹⁾ Additionally, with the discovery of new pollutants and a deeper understanding of their impacts on human health, the adequacy of the AQI evaluation system for comprehensively covering various pollutants is still worth exploring.⁽¹²⁾

Factors such as urban form, land use, road transportation, and ecological environment impact the respiratory health of urban populations by influencing the human living environment and behavior.^(13,14) The compact urban development approach in China has increased the density of population distribution, thereby reducing the total amount of pollutant emissions and increasing the degree of exposure to spatially pathogenic environments.⁽¹⁵⁾ The urban built environment, land use status, and urban form structure affect the concentration distribution of air pollutants; a compact urban form can increase the pedestrian use of streets and improve the efficiency of public transportation, thereby reducing the amount of vehicle emissions and road particulate pollution.⁽¹⁶⁾ Building height, massing, layout, and orientation can have important effects on the flow and distribution of air pollution. Urban planning can promote health by reducing the impact of pollution on the human body and promoting physical activity.⁽¹⁷⁾ In urban construction, the urban spatial environment should be optimized to mitigate air pollution through a coordinated layout. Note that previous studies have mostly focused on the effect of pollutants on respiratory diseases from an epidemiological perspective or the effect of the spatial environment on the diffusion and distribution of pollutants from an ecological perspective, but studies on the mechanisms of respiratory pathogenesis from a spatial perspective are relatively few.⁽¹⁸⁾ The results of these studies ignore the mutual spillover and effects of urban spatial environmental indicators, suffer from model estimation bias, and often underestimate the effects of spatial environmental indicators on respiratory health. Therefore, the research findings often lack guidance for urban construction.

In this study, we applied air pollution remote sensing monitoring data and combined them with population thermal data and applied a risk exposure evaluation model to study the spatial distribution pattern of respiratory health risks in Shenyang. We also applied geographical detection methods to assess the correlation between spatial environmental elements and risk space. This paper has three main objectives: (1) to evaluate the spatial distribution of current respiratory risks, (2) to identify the main spatial environmental factors affecting respiratory health risks and analyze their spatial autocorrelation, and (3) to explore the joint effects of potential factors on respiratory health risks. By achieving these objectives, we aim to provide valuable insights for policymakers and public health officials to develop targeted interventions and strategies to mitigate respiratory health risks in urban environments.

2. Materials and Methods

2.1 Study area

The city of Shenyang (41° 48' 11.75"N, 123° 25'31.18"E) is located in the central part of Liaoning Province, covering an area of about 12860 km². It has a temperate monsoon climate

with an average annual temperature of 6.2–9.7 °C and four distinct seasons. The annual precipitation is approximately 600–800 mm, with rainfall concentrated mainly in summer. Since its reform and opening up, Shenyang has played a pioneering role in the industrial development of China. The acceleration of urbanization has indirectly led to increased air pollution. Moreover, the number of deaths from respiratory, cardiovascular, and cerebrovascular diseases has increased in line with the rising concentrations of air pollutants. The urban area of this study is primarily the central area of Shenyang, involving eight administrative districts in which approximately 68% of the region's population is concentrated, with a total area of approximately 454.05 km² (Fig. 1).

2.2 Research methods

2.2.1 Air quality assessment based on respiratory health

The United States was the first to establish ambient air index standards in the 1970s. Subsequently, other countries established their own air quality index systems based on their air quality conditions, such as China's Air Pollution Index and AQI. AQI is calculated by listing the concentration limits against each pollutant and taking the maximum IAQI for each pollutant to determine AQI.⁽¹⁹⁾ This calculation method has an unclear basis for grading air pollutant concentration breakpoints and does not reflect the true overall characteristics of current air quality. Proper air quality management requires a reliable air quality classification system; however, the classification standards vary from country to country, and the blurring of air quality boundaries affects the accurate evaluation of air quality.

Fuzzy theory was developed on the basis of the fuzzy set theory formulated by L.A. Zadeh of the Department of Electrical Engineering at the University of California, Berkeley, USA, in 1965.⁽²⁰⁾ Fuzzy logic specializes in expressing qualitative knowledge and experience with unclear boundaries. It can distinguish fuzzy sets, deal with fuzzy relationships, and simulate the human brain to realize rule-based reasoning.⁽²¹⁾ Therefore, some scholars have applied it to air quality assessment methods to solve the problem of overly arbitrary air pollutant concentration grading. Onkal-Engin *et al.*⁽²²⁾ applied fuzzy algorithms to assess urban air quality in Istanbul, and they confirmed that fuzzy algorithms are very suitable for air quality management. However, owing to the lack of data support for the classification and determination of weight coefficients of air pollutants, the calculation results of fuzzy algorithms can only represent the comprehensive trend of air pollution degree and cannot express the true pathogenic degree of air pollution.⁽²³⁾ In this study, we summarize the air quality standards issued by the World Health Organization⁽⁷⁾ and the Chinese government based on the degree of impact of air pollutants on human respiratory health, form air quality standards for respiratory health, and formulate a reliable classification system for air pollution concentrations. A comprehensive fuzzy assessment method was established to eliminate the effects of blurred air quality boundaries. Fuzzy comprehensive assessment can be divided into three stages.

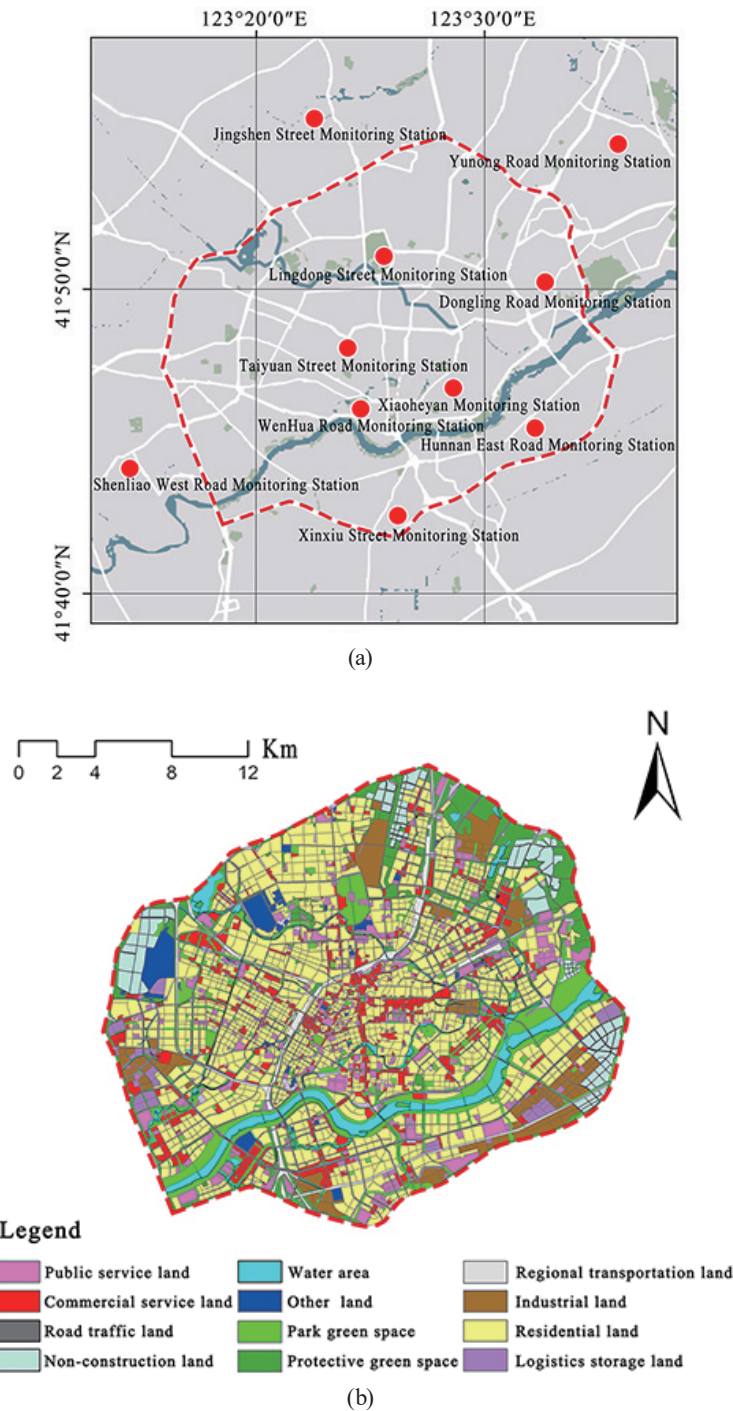


Fig. 1. (Color online) Study area. (a) Distribution of air quality monitoring stations in Shenyang. (b) Layout map of the Third Ring Road in Shenyang.

(1) Constructing a fuzzy affiliation function

In this study, we comprehensively referenced the latest global air quality guidelines issued by the WHO and the pollutant concentration limits defined in the Chinese national environmental

protection standard [Technical Regulation on the Ambient Air Quality Index (on trial)]. We classified eight levels of air quality standards (Table 1), and the lower the level, the higher the air quality and the more notable the negative effects on human respiratory health (Fig. 2).

The value of the fuzzy affiliation function for each of the factors associated with the eight assessment levels can be calculated using the following set of equations:

$$\begin{aligned}
 \mu_A &= \begin{cases} 1, & 0 \leq x \leq D_A \\ \frac{D_B - x}{D_B - D_A}, & D_A \leq x \leq D_B \\ 0, & x \geq D_B \end{cases} & \mu_B &= \begin{cases} 0, & x \leq D_A \text{ or } x \geq D_C \\ \frac{x - D_A}{D_B - D_A}, & D_A < x < D_B \\ 1, & x = D_B \\ \frac{D_C - x}{D_C - D_B}, & D_B < x < D_C \end{cases} \\
 \mu_C &= \begin{cases} 0, & x \leq D_B \text{ or } x \geq D_D \\ \frac{x - D_B}{D_C - D_B}, & D_B < x < D_C \\ 1, & x = D_C \\ \frac{D_D - x}{D_D - D_C}, & D_C < x < D_D \end{cases} & \mu_D &= \begin{cases} 0, & x \leq D_C \text{ or } x \geq D_E \\ \frac{x - D_C}{D_D - D_C}, & D_C < x < D_D \\ 1, & x = D_D \\ \frac{D_E - x}{D_E - D_D}, & D_D < x < D_E \end{cases} \\
 \mu_E &= \begin{cases} 0, & x \leq D_D \text{ or } x \geq D_F \\ \frac{x - D_D}{D_E - D_D}, & D_D < x < D_E \\ 1, & x = D_E \\ \frac{D_F - x}{D_F - D_E}, & D_E < x < D_F \end{cases} & \mu_F &= \begin{cases} 0, & x \leq D_E \text{ or } x \geq D_G \\ \frac{x - D_E}{D_F - D_E}, & D_E < x < D_F \\ 1, & x = D_F \\ \frac{D_G - x}{D_G - D_F}, & D_F < x < D_G \end{cases} \\
 \mu_G &= \begin{cases} 0, & x \leq D_F \text{ or } x \geq D_H \\ \frac{x - D_F}{D_G - D_F}, & D_F < x < D_G \\ 1, & x = D_G \\ \frac{D_H - x}{D_H - D_G}, & D_G < x < D_H \end{cases} & \mu_H &= \begin{cases} 0, & 0 \leq x \leq D_G \\ \frac{x - D_G}{D_H - D_G}, & D_G < x < D_H \\ 1, & x \geq D_H \end{cases}
 \end{aligned} \tag{1}$$

where μ_{A-H} is the fuzzy affiliation function, x is the average annual air pollutant monitoring value, and D_{A-H} is the average annual air quality classification value.

(2) Building a fuzzy relationship matrix

The assessment matrix R can be obtained from the affiliation values of the input pollutant values and the corresponding air quality parameters.

Table 1
Annual average air quality evaluation criteria.

	Standard level	SO ² (ug/m ³)	NO ² (ug/m ³)	O ³ (ug/m ³)	CO (mg/m ³)	PM _{2.5} (ug/m ³)	PM ₁₀ (ug/m ³)
D _A	Level 1 (≤ 50)	20 [□]	10 [◊]	60 [◊]	1 [◊]	5 [◊]	15 [◊]
D _B	Level 2 (> 50 and ≤ 100)	60 [□]	20 [◊]	70 [◊]	2 [◊]	10 [◊]	20 [◊]
D _C	Level 3 (> 100 and ≤ 150)	100 [□]	30 [◊]	100 [◊]	4 [◊]	15 [◊]	30 [◊]
D _D	Level 4 (> 150 and ≤ 200)	140 [◊]	40 [◊]	160 [◊]	7 [◊]	25 [◊]	50 [◊]
D _E	Level 5 (> 200 and ≤ 250)	220 [◊]	70 [◊]	200 [◊]	12 [◊]	35 [◊]	70 [◊]
D _F	Level 6 (> 250 and ≤ 300)	300 [◊]	100 [◊]	300 [◊]	18 [◊]	75 [◊]	150 [◊]
D _G	Level 7 (> 300 and ≤ 350)	400 [◊]	160 [◊]	400 [◊]	24 [◊]	150 [◊]	200 [◊]
D _H	Level 8 (> 350)	800 [◊]	250 [◊]	800 [◊]	30 [◊]	250 [◊]	300 [◊]

Note: ◊: Indicator from the Global Air Quality Guideline (2021); □: Indicator from the Chinese national standard ambient air quality standards (GB 3095—2012); ◊: Indicator based on daily average values calculated on a pro rata basis.

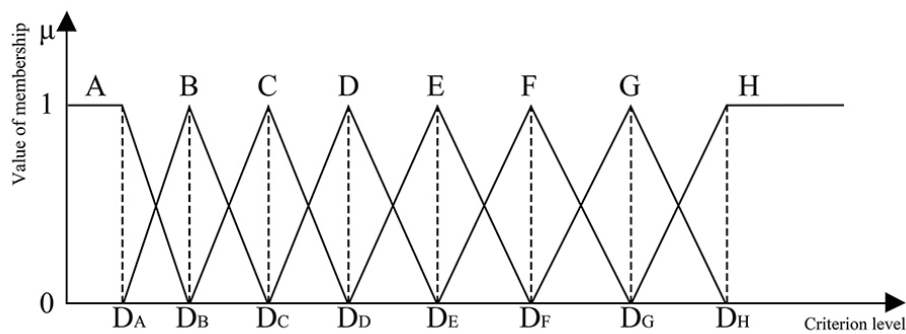


Fig. 2. Fuzziness for fuzzy classification method. μ : fuzzy membership degree; A–H: fuzzy membership level; D_A–D_H: concentration classification of air pollutants.

$$R = \begin{bmatrix} r_{11} & r_{12} & \dots & r_{18} \\ r_{21} & r_{22} & \dots & r_{28} \\ r_{31} & r_{32} & \dots & r_{38} \\ r_{41} & r_{42} & \dots & r_{48} \\ r_{51} & r_{52} & \dots & r_{58} \\ r_{61} & r_{62} & \dots & r_{68} \end{bmatrix} \tag{2}$$

$$r_{ij} = \mu_j(x), i = 1, 2, \dots, 6, j = 1, 2, \dots, 8$$

$$\{\mu_1, \mu_2, \mu_3, \mu_4, \mu_5, \mu_6, \mu_7, \mu_8\} = \{\mu_A, \mu_B, \mu_C, \mu_D, \mu_E, \mu_F, \mu_G, \mu_H\}$$

The fuzzy matrix can be solved according to the maximum subordination principle.

$$A_i = \max \{r_{i1}, r_{i2}, r_{i3}, r_{i4}, r_{i5}, r_{i6}, r_{i7}, r_{i8}\}, i = 1, 2, \dots, 6 \tag{3}$$

$$A = \{A_1, A_2, A_3, A_4, A_5, A_6\} = \{A_{SO_2}, A_{CO}, A_{NO_2}, A_{O_3}, A_{PM_{2.5}}, A_{PM_{10}}\}$$

Here, A_i is the standard level and A_i is an integer from 1 to 8. If $r_{ij} = r_{ij'}$ and $j < j'$, then A_i equals j' corresponding to the standard level grade value.

The overall air pollution status cannot be determined via individual pollutants; each pollutant contributes to air pollution in some way. In this study, we collated relevant findings on the relationship between air pollutant concentrations and respiratory disease outpatient visits in Shenyang and cities at the same latitude; the effects of air pollutants on respiratory health could be ranked as follows:^(24–26) $\text{CO} > \text{NO}_2 > \text{SO}_2 > \text{PM}_{2.5} > \text{PM}_{10} > \text{O}_3$. The weighting coefficients for the effects of each type of air pollutant on respiratory health were further calculated via hierarchical analysis.

The weighting factor matrix can be obtained as

$$W = \{w_{\text{SO}_2} (0.16), w_{\text{CO}} (0.36), w_{\text{NO}_2} (0.28), w_{\text{O}_3} (0.04), w_{\text{PM}_{2.5}} (0.09), w_{\text{PM}_{10}} (0.07)\}. \quad (4)$$

(3) Establishing a fuzzy integrated evaluation algorithm model

Fuzzy integrated evaluation results can be obtained as

$$B = W * A = (b_1, b_2, b_3, b_4, b_5, b_6), b_i = A_i * w_i, i = 1, 2, \dots, 6, \quad (5)$$

$$\text{Class} = b_1 + b_2 + b_3 + b_4 + b_5 + b_6.$$

2.2.2 Respiratory health exposure risk assessment of air pollution

Currently, the generally accepted tool for assessing the effects of environmental factors on the human body is the risk assessment method. This method is used by leading scientists in the field of hygiene and epidemiology to study and evaluate the effects of various etiological substances on human health. The study of the effects of major atmospheric pollutants on human health is carried out mainly through two aspects. The first is through the uninterrupted monitoring of individuals for specific time periods and the evaluation of the risks posed by pollutants based on this monitoring to obtain data on the doses of pollutants inhaled by humans, which are combined with physical health data.⁽²⁷⁾ The second involves the study of the stagnation time of major air pollutants in the spatial environment, combined with the degree of population concentration, to evaluate the effects of major air pollutants on human health. The second method is currently the most common method of evaluating the impact of pollutants on human health. Spatial simulation methods are used to simulate the spatial distribution of pollutants and thus more accurately evaluate the effects of major air pollutants on human respiratory health. We applied a method to assess the risk status of the respiratory health of the population with long-term exposure to air pollutants. The urban atmospheric conditions were evaluated according to the priority pollutants of the surface layer of the atmosphere – sulfur dioxide, nitrogen dioxide, carbon monoxide, ozone, and suspended solids – and the results of the gas evaluation were then combined with the population distribution to assess the population's risk of respiratory exposure.⁽²⁸⁾ We used this exposure risk evaluation model to reflect the quantitative population respiratory health risk, which can distinguish the severity of local areas relative to the spatial whole. We cited the population exposure risk model equation.

$$R_{ij} = \frac{pop_{udc} \times C_{ij}}{\sum_{i=1}^n pop_{udc} \times \frac{C_{ij}}{n}} \quad (6)$$

In this equation, i is the grid number and j is the characteristic type of air pollution source (e.g., industrial source). R_{ij} denotes the relative risk of air pollution exposure of the population in grid i with the contribution of type j sources. pop_{udc} is the number of people in a single grid of urban land-use type u in spatial cell d . C_{ij} is the pollution concentration of grid i under the contribution of type j sources. n is the total number of grids contained in spatial cell C .

2.2.3 Correlation analysis

In this study, a geodetector was used to test the relationship between the role of spatial environmental factors and exposure risk. It is a statistical method that primarily detects spatial heterogeneity and is applicable to the spatial geographic analysis of driving forces, which can integrate the homogeneity and variability of the distribution of environmental elements and high-risk spaces and better relate environmental factors to high-risk spaces for quantitative assessment.⁽²⁹⁾ In this study, we used three main methods, Pearson's correlation coefficient, factor detection, and interaction detection, to investigate the correlation between spatial environmental factors and exposure risk.

(1) Factor detection analyzes whether there is significant similarity in spatial distribution by testing the spatial divergence between the dependent and independent variables; if the two show spatial similarity, it means that the element in question plays a considerable role in the formation of spatial changes in the geographical element. The formula is

$$q = \frac{1 - \sum_{h=1}^L N_h \sigma_h^2}{N \sigma^2} \quad 1 - \frac{SST}{SST} \quad (7)$$

In this formula, h is the stratification of factor X ; N_h is the number of cells in layer h ; N is the total number of cells in the whole region; the q value is between 0 and 1. The more similar the spaces of the independent variable X and the dependent variable Y are, the greater their effect on the dependent variable Y and the greater the q value, and vice versa.

(2) Pearson's correlation coefficient quantifies the linear relationship between two variables by calculating their covariance and standard deviation. Its value ranges from -1 to 1 , with 1 indicating a perfect positive correlation, -1 indicating a perfect negative correlation, and 0 indicating no linear relationship. The formula is

$$r = \frac{\sum (X_i - \bar{X})(Y_i - \bar{Y})}{\sqrt{\sum (X_i - \bar{X})^2 \sum (Y_i - \bar{Y})^2}} \quad (8)$$

In this equation, r is Pearson's correlation coefficient, which reflects the degree of linear correlation between two variables. X_i is the i th data point of variable X . Y_i is the i th data point of variable Y . \bar{X} is the mean of variable X . \bar{Y} is the mean of variable Y .

(3) Interaction detection involves identifying the interactions between various variables. It assesses whether the combined effect of factors X_1 and X_2 enhances or diminishes their explanatory power on the dependent variable, or if these factors independently influence the dependent variable. The assessment is performed by calculating the effect of each spatial environmental factor on the risk, examining each effect when these factors interact, and then comparing the magnitude of the effect among the three factors.

2.3 Data acquisition

2.3.1 Air quality data

The air pollutant data used in this paper were obtained from the China High Air Pollutants (CHAP) dataset and the Shenyang Environmental Monitoring Centre (EMC). The air pollutants include SO_2 , NO_2 , CO , O_3 , PM_{10} , and $\text{PM}_{2.5}$. The CHAP dataset refers to the long-term, full-coverage, high-resolution, and high-quality datasets of ground-level air pollutants in China. It is generated from the big data (e.g., ground-based measurements, satellite remote sensing products, atmospheric reanalysis, and model simulations) using artificial intelligence by considering the spatiotemporal heterogeneity of air pollution.^(30,31) The CHAP dataset has an accuracy of 1 km for $\text{PM}_{2.5}$, PM_{10} , O_3 , and NO_2 , and an accuracy of 10 km for SO_2 and CO . We used the monitoring data from the EMC for the accuracy correction of the six categories of air pollutants. There are 10 monitoring stations distributed within the city of Shenyang; the temporal resolution is hour-by-hour, and the time span collected was from January 1 to December 31, 2019, for a total of 1095728 data messages. The spatial interpolation method for anti-weight distance was selected to design a calculation scheme based on sampling data, and an air pollution trend surface with a spatial resolution of $500 \times 500 \text{ m}^2$ was generated.

2.3.2 Land use data

The 2019 remote sensing image data of Shenyang used in this paper were obtained from the Geospatial Data Cloud website. The remote sensing data were interpreted by the Envi method. A total of 12 classes of land use types were identified: public management and services, business services, facilities, water sources, other nonconstruction land areas, water and other land areas, park green space, protective greenbelt, regional facilities, industrial, residential, and traffic facilities, and logistics warehousing. The general integration of various land types resulted in eight types of land use: water sources and water areas were classified as water area land; park green space and protective greenbelts were classified as green land; regional transportation facilities and associated land were classified as land for transportation facilities (Fig. 1).

2.3.3 Population distribution data

We obtained the population thermal data of the $500 \times 500 \text{ m}^2$ area of Shenyang through cell phone signaling data. The mobile signaling data used in this study were from China Unicom Smart Footprint Data Technology Co., Ltd., which was the first batch of population big data officially purchased by the Ministry of Natural Resources of China in 2019. The data in this study were selected from the typical months of each season (January, April, July, and September), from which three typical days were selected (two working days and one holiday) to analyze the spatial and temporal distribution characteristics of the population within the Third Ring Road of Shenyang in each season (Fig. 3).

2.3.4 Spatial environmental element data

Numerous studies have demonstrated that regulating some urban spatial environmental factors can improve the current situation of air pollutant concentrations. The role of the urban spatial environment in air pollution is reflected mainly in four spatial environmental factors, which can exert direct impacts on human respiratory health within the city: land use, spatial morphology, road traffic, and green and open spaces. In this study, 25 spatial environmental factors were selected. A map of the spatial environmental factors with $500 \text{ m} \times 500 \text{ m}$ resolution was obtained by interpreting the land use data (Table 2).

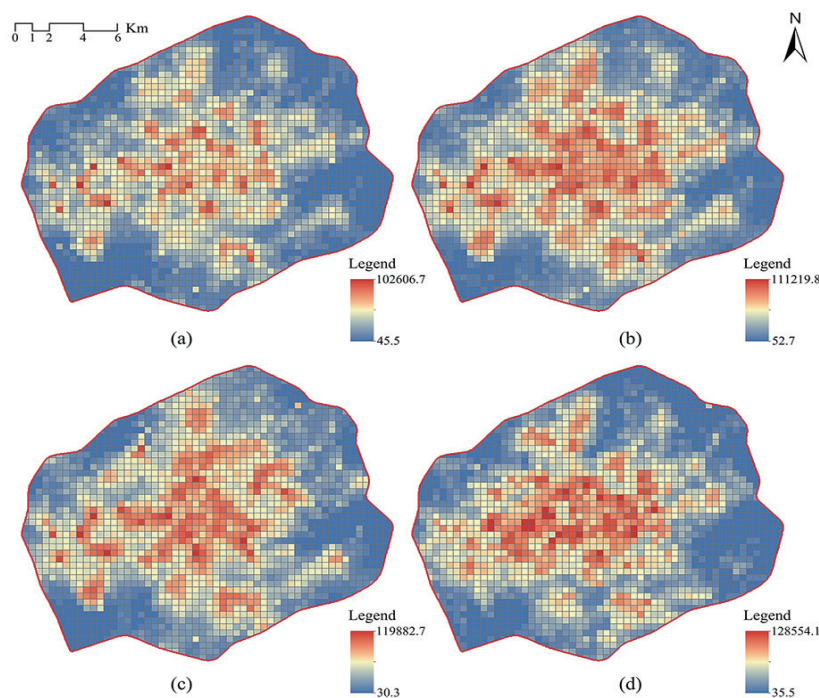


Fig. 3. (Color online) Spatial and temporal distributions of population in different seasons in the Third Ring Road of Shenyang in 2019: (a) spring, (b) summer, (c) autumn, and (d) winter.

Table 2
List of selected urban spatial environmental factors.

Category	Detailed categories	Abbreviation	Description
Land use	Percentage of public service land area	PLA	Percentage of area of each type of land use per unit area
	Percentage of commercial land area	CLA	
	Percentage of residential land area	RLA	
	Percentage of industrial land area	ILA	
	Percentage of logistics and warehousing land area	LLA	
	Percentage of land area for transportation facilities	TLA	
	Percentage of green space	GLA	
	Percentage of water area	WLA	
Spatial form	Intensity of land development	LDI	Ratio of total construction land to urban area
	Building density	BUD	Ratio of total base area of building to occupied land area within certain area
	Volume ratio	VOR	Ratio of total above-ground floor area to site area
	Sky openness	SOD	Quantitative description of degree of openness of urban form
	Roughness length	RLD	Height when air flow is subjected to rough element resistance of ground.
	Ventilation potential factor	VPF	Urban ventilation capacity
Road traffic	Road area ratio	RAR	Ratio of total urban road land area to total area
	Density of primary road network	PRD	Ratio of total centerline length of trunk roads to total site area
	Density of secondary road network	SRD	Ratio of total centerline length of secondary roads to total site area
	Transportation coverage	BLD	Number of bus stops within 500 m of travel space
	Density of bus stops	BSD	Sum of the service areas covered by bus stops within 500 m
Green open space	Green space coverage ratio	GSR	Ratio of total area of each green area in built-up area to total area of built-up area
	Patch density	PD	Number of patches per unit area
	Aggregation index	AI	Degree of aggregation of different patch types in landscape
	Landscape shape index	LSI	Complexity in spatial pattern of shapes used to measure landscape types
	Landscape division index	DIVISION	Degree of fragmentation of landscape patches
	Number of patches	NP	Number of patches of landscape type

3. Results and Discussion

3.1 Differences in spatial and temporal distributions of health risks

The distribution of human respiratory health risks in the core built-up area of Shenyang is shown in Fig. 4. In terms of spatial distribution patterns, the spatial heterogeneity of urban respiratory health risks was large, with an overall trend showing risk gradually decreasing from the center outwards. The health risk safety areas were distributed mainly in areas with rich

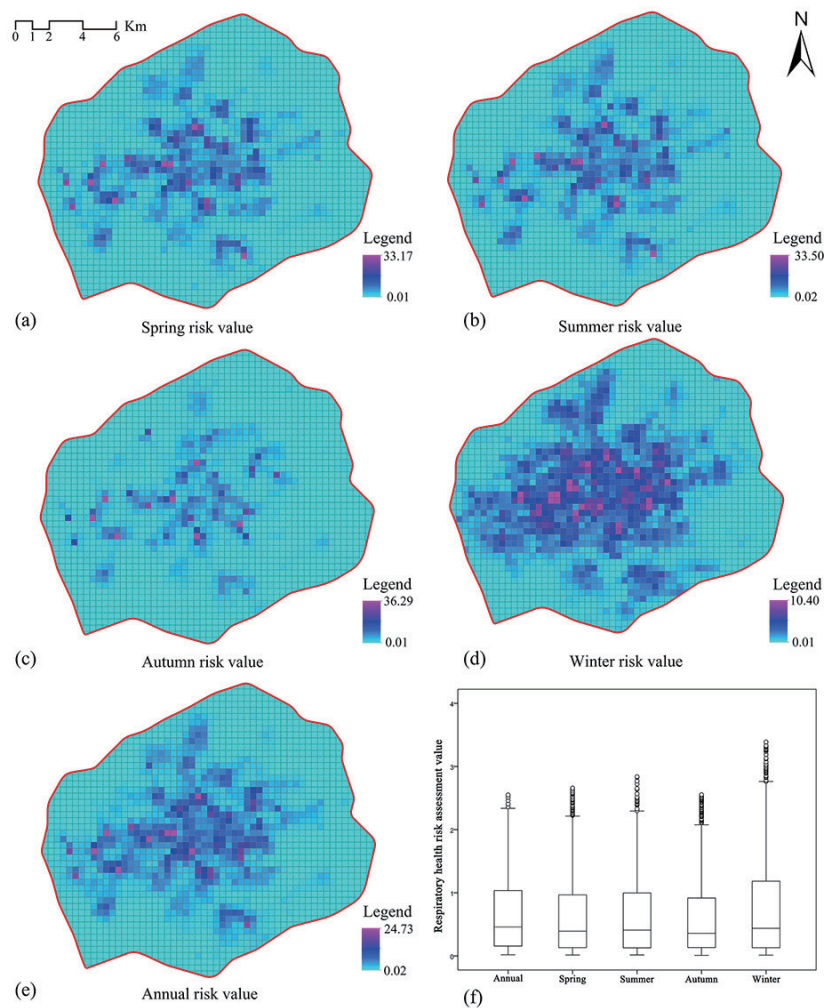


Fig. 4. (Color online) Spatial distribution of respiratory health risks by season and year in the core area of Shenyang in 2019.

natural ecological spaces at the periphery of the city; areas with higher health risk were scattered in the central areas of the city, primarily around major commercial and high-density residential areas. Natural ecological space and respiratory health risk in the city showed similar distribution patterns; the value of health risk was lower in areas with higher urban vegetation coverage and more open space. In terms of time variation (Fig. 4), respiratory health risks in Shenyang showed significant seasonal spatial distribution differences, although they demonstrated the same trend in spring and summer. The high-risk area was slightly lower in summer than in spring, with the main health risk areas scattered in the urban core. The range and location of health risks in autumn were significantly different from those in spring and summer. The range of respiratory health risks in autumn was the smallest, accounting for 6.87% of the total area. The high-risk areas were scattered and concentrated in the urban center. In winter, the range of the respiratory health risk index was the smallest, and the highest risk index was 10.4. However, the range of respiratory health risk in winter was the highest throughout the year, and the high-risk areas were concentrated and distributed in the urban center.

Shenyang respiratory health risks showed strong spatial and temporal heterogeneities. This phenomenon may be caused by changes in human activities, spatial environment, and meteorological conditions. Meteorological factors in the study area show a clear seasonal variation, as the study area was located in the temperate monsoon region in northeastern China. Thus, seasonal changes under urban meteorological conditions also affect the temporal variability of respiratory health risks. The dominant wind directions in Shenyang are southeastern in summer and northwestern in winter. In winter, numerous inhalable particles are brought from the Loess Plateau, leading to an increased pollutant concentration in these seasons. Shenyang has a long and cold winter, with a total of five months of heating time throughout the year. Pollutant concentration is generally higher in winter and early spring than in other seasons due to coal-fired heating.⁽³²⁾ In addition, the large temperature difference between day and night at high latitudes and the clear atmospheric temperature inversion also provide favorable conditions for the easy accumulation and diffusion of pollutants.⁽³³⁾ Urban green space and water bodies exert important effects on atmospheric pollutants and can also adjust the microclimate environment.⁽³⁴⁾ The purification effect of urban vegetation and water bodies is the strongest in the summer, resulting in the best air quality; in contrast, the purification effect of urban vegetation and water bodies has a weak effect in winter, leading to the worst air quality.⁽³⁵⁾ Our study demonstrated that land use, spatial morphology, road transportation, and green open space all play important roles in respiratory health risks. The urban spatial environment can change the local spatial microclimate environment, thereby affecting the city's local air pollution.⁽³⁶⁾ The urban spatial environment is also an important source of urban air pollution, and its layout has a direct effect on respiratory health risks.⁽³⁷⁾ Urban industrial, traffic, and individual building spaces are all important sources of air pollution.⁽³⁸⁾ Therefore, the layout of such spaces can lead to spatial variability in air pollution. Eastern Shenyang houses the Chipanshan Ecological Protection Area. The density of urban population and green space area gradually increase from the center outwards, which is one of the main reasons for the temporal difference of air quality and health risk.

In addition, high-risk areas of respiratory health are affected not only by air pollutants but also by population concentration.⁽³⁹⁾ The results of respiratory health risk evaluation showed that the highest risk value was much lower in winter (10.40) than in the other three seasons (approximately 30). Compared with the other seasons, the statistical data of the population distribution in winter reflect that the winter population decreased by 1 million, mainly caused by migration during the Chinese Spring Festival. The average risk values of the four seasons were similar. Therefore, we found that the health risk in winter was still the most serious. The urban spatial environment and urban land use functions will affect the spatial flow and distribution of the population.⁽⁴⁰⁾ Areas with poor atmospheric conditions and high population density tend to exhibit higher respiratory health risks.

3.2 Effectiveness of risk factors

We first calculated the correlation coefficients (Pearson coefficients) between each spatial environmental element and spatial risk values by using the function of multiple stepwise

regression analysis to measure the effectiveness of the selection of spatial environmental elements. The results showed that there was a correlation between the respiratory health risk space and 23 spatial environmental factors in Shenyang (Table 3). The correlation coefficient values between the annual risk value and the percentage of logistics land area and the percentage of primary road network density were close to 0, and the p -value was greater than 0.05, thus indicating that there was no correlation between the annual risk value and the two factors. Therefore, these two factors were excluded from subsequent measurements.

The factor detector of the geodetector revealed the extent to which spatial environmental factors explain the variation in respiratory health risk. The factor detector showed the following results (Table 3). In terms of land use, only the percentage of residential land area showed a strong correlation with respiratory health risk, with an explanatory power of 11% for the risk; the percentage of green space area showed a more general correlation with respiratory health risk, with an explanatory power of 6.4%; the percentage of other land area showed a weak correlation effect with respiratory health risk, indicating that, in terms of urban land use, only the percentage of other land areas showed a weak correlation with respiratory health risk. These results indicate that only residential land use and green areas have a significant effect on respiratory health risk. In terms of urban spatial morphology, all spatial environmental elements showed significant correlations. The volume ratio and sky openness had the strongest explanatory power for respiratory health risk, explaining 26.9 and 25.3% of the risk variation, respectively, indicating that urban spatial morphology is a key factor affecting respiratory health risk. In terms of road traffic, the road area ratio showed a weak correlation with respiratory health risk, with an explanatory power of 2.4% of the risk; there was a general correlation between respiratory health risk and SRD, BLD, and BSD, with explanatory powers of 6.8, 6, and 6.4%, respectively. In terms of urban green open space elements, the green space coverage ratio showed a general correlation with respiratory health risk, with an explanatory power of 6.4%. The remaining spatial indicators showed a strong correlation with respiratory health risk, with an explanatory power of approximately 10% for each indicator.

Table 3
Pearson correlation analysis results and factor detection results.

Project	Pearson correlation	q value	Project	Pearson correlation	q value
PLA	0.063**	0.02	VPF	0.196**	0.118
CLA	0.138**	0.037	RAR	0.092**	0.024
RLA	0.319**	0.115	PRD	0.001	—
ILA	-0.097**	0.011	SRD	-0.183**	0.068
LLA	-0.036	—	BLD	0.258**	0.06
TLA	0.092**	0.024	BSD	0.243**	0.066
GLA	-0.237**	0.064	GSR	-0.237**	0.064
WLA	-0.193**	0.042	PD	-0.324**	0.104
LDI	0.267**	0.079	AI	-0.277**	0.094
BUD	0.307**	0.138	LSI	-0.313**	0.113
VOR	0.509**	0.269	DIVISION	-0.102**	0.107
SOD	-0.464**	0.253	NP	-0.324**	0.108
RLD	0.151**	0.102			

Note: $p > 0.05$, $*p < 0.05$, $**p < 0.01$. The p -value values were all less than 0.001.

According to the spatial autocorrelation analysis, the percentage of logistics land area and the density of the primary road network did not correlate with the annual risk value; this is mainly due to urban management constraints, as logistics land is not deployed within the Third Ring Road, which exerts a substantial impact on the quality of the air environment. Previous studies have shown that primary road networks are both an important source of urban traffic pollution and also an important urban corridor for the exclusion of air pollutants;⁽⁴¹⁾ thus, the density of the primary road network is not an important factor affecting the risk level.

Related studies have shown that urban land expansion significantly affects air pollution, with higher levels of air pollution in areas with higher levels of urban land development.⁽⁴²⁾ Wang *et al.* suggested that the spatial structure of cities with high population density caused an inverted U-shaped change in air pollution based on the statistics of 194 prefecture-level cities in China, and in the eastern part of China, residential land, public facilities land, and transportation land in the urban structure had the greatest impact on air pollution.⁽⁴³⁾ This is consistent with the findings of our study. In addition, RAR, BLD, and BSD also had positive effects on respiratory health risk, but with a lower intensity than land use and spatial pattern; this indicates that road traffic is an important source of air pollutants, but it accounts for a relatively small proportion of all pollutants. This finding was verified in a study by Harrison *et al.*⁽⁴⁴⁾

The layout, scale, and vegetation configuration of green spaces help to form urban ventilation corridors, purify air, absorb dust, and improve air quality in urban areas,⁽⁴⁵⁾ thereby affecting public respiratory health; this is consistent with our findings. We found that an increase in the density of urban secondary road networks reduced the respiratory health risk throughout the year, which is consistent with the results of previous studies that small neighborhoods and dense road networks can effectively mitigate urban air pollution.⁽⁴⁶⁾ The results indicated that sky openness had the strongest negative effect on risk. This may be because the higher the sky openness of a region, the easier it is for clean airflow from the periphery to enter the interior of the city, and the easier it is to expel the internal polluted air to the periphery of the city. In contrast, a higher volume ratio brings an excessive population concentration, and a high level of site development will reduce the sky openness of the region, thereby increasing air pollution.⁽⁴⁷⁾

3.3 Interaction of risk factors

Interaction detection was used to detect whether two potential factors interacted with each other. The detection results showed that each spatial environmental element variable enhanced its own effect on respiratory health risk to some extent after interaction. Interaction detection determined the interaction effects between pairs of factors. We measured the positive and negative effects of spatial environmental factors on respiratory health risk separately.

The results of measuring the factors with positive effects on respiratory health risk (Fig. 5) showed three interaction effects: “enhanced, nonlinear”, “enhanced, two-factor variable”, and “single-factor nonlinear weakening”. The first and second scenarios imply that the joint effect of two factors on respiratory health risk is greater than the effect of two independent factors. Therefore, for any two factors other than the volume ratio factor in this study, their combined effects on respiratory health risk were stronger than those considered independently. We found a

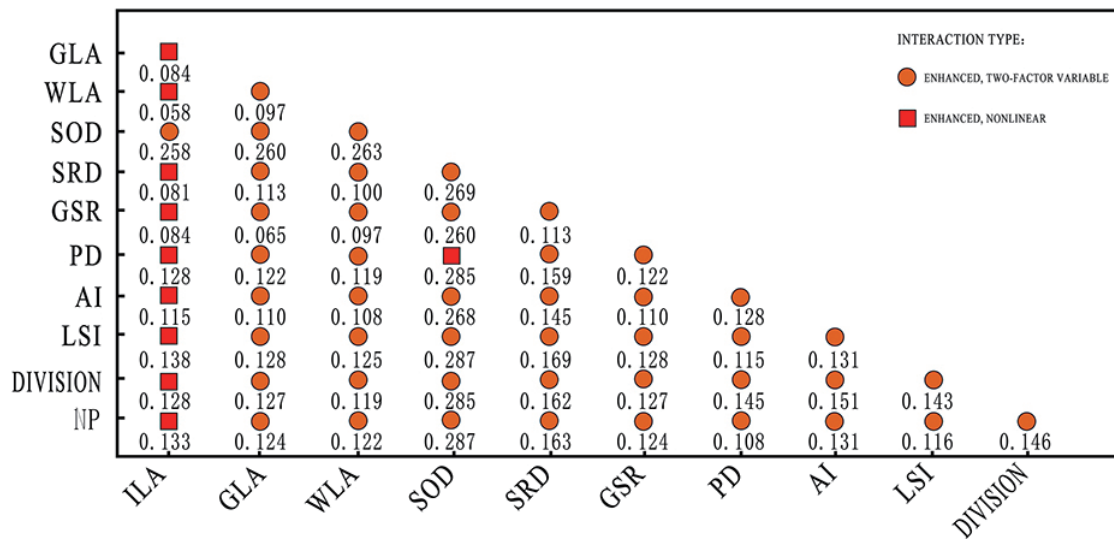


Fig. 5. (Color online) Results of spatial environmental interaction detection of positive effects.

stronger effect of an increasing mix of urban functional land use categories on respiratory health risk. For example, the interaction of PLA ($q = 0.020$) and CLA ($q = 0.037$) nonlinearly increased respiratory health risk, with a q value of 0.060 after the interaction, and the interaction results of other types of land use showed similar results. This finding may be explained by the fact that when different types of land use are functionally mixed, population movement within the area increases, leading to multiple population concentrations and a subsequent rise in air pollutant levels from human activities.⁽⁴⁸⁾ BLD and BSD had a small effect on their own but a large interaction with other factors. For example, the interaction of BSD ($q = 0.066$) and TLA ($q = 0.024$) nonlinearly increased respiratory health risk ($q = 0.110$). There could be two potential reasons for this. One is that roads are an important source of pollution in the region, and public transportation is usually located along major urban roads; the other is that a developed public transportation system results in the concentration and mobility of people in space; when these two factors are combined, respiratory health risk is significantly enhanced.⁽⁴⁹⁾ In this study, we also found that the interaction results of the floor area ratio factor with other land area share factors showed a nonlinear weakening trend. For example, the interaction result of VOR ($q = 0.296$) and PLA ($q = 0.020$) had a q value of 0.278. The reason for this phenomenon may be that, on the one hand, land with a high plot ratio will increase the number of people within the land, resulting in increased respiratory health risk. On the other hand, land with a high plot ratio will have a larger building height and a lower building density, which will increase the green space area within the land and improve the ventilation state of the land.⁽⁵⁰⁾ The interaction between volume ratio and road area ratio showed a nonlinear weakening trend, confirming the mitigating effect of “small neighborhoods and dense road networks” on respiratory health risk.

The results of the measurement of the factors with negative effects on respiratory health risk (Fig. 6) showed two interaction effects: “enhanced, nonlinear” and “enhanced, bivariate”. The interaction between ILA and SOD was greater than the single q value of the two factors

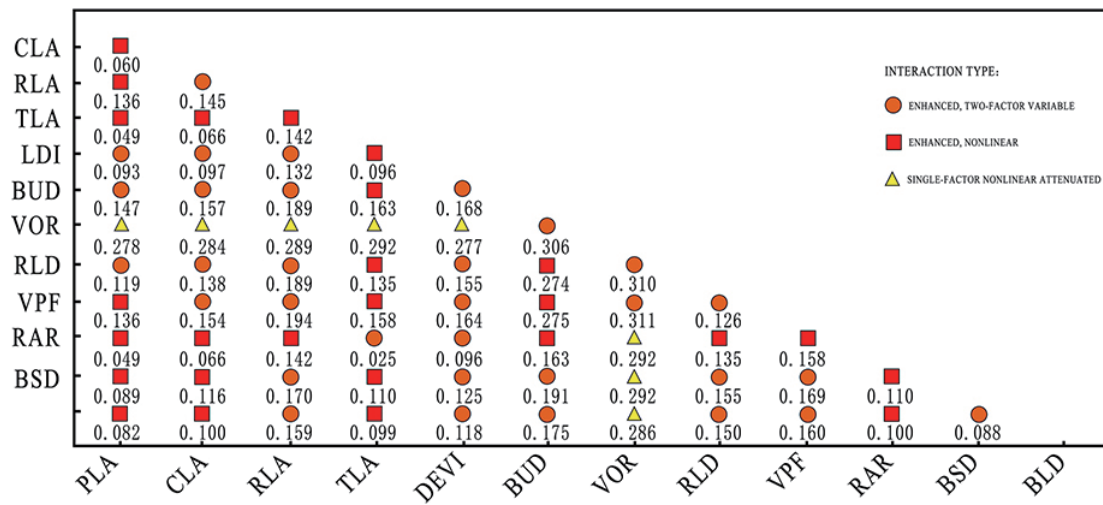


Fig. 6. (Color online) Results of spatial environmental interaction detection of negative effects.

separately and weaker than the sum of the two individual effects, resulting in an enhanced two-factor variable. The interaction between ILA and other factors with negative effects was greater than the sum of the two individual effects, resulting in an enhanced nonlinear interaction effect. The interaction between PD and SOD was enhanced and nonlinear, whereas the interaction between any other negative effectors was enhanced and bivariate. Therefore, the interaction for any two factors in the study had a stronger effect than their independent effects. The interaction results of factors such as the proportion of industrial land and green space in Shenyang showed nonlinear enhancement; the reason for this may be that industrial land (clean, unpolluted industrial land) within the city is characterized by low building density, low building height, and good greenness. The results showed an enhanced bivariate interaction of various factors of green space and water bodies. Previous studies have shown that green space and water body factors impact respiratory health in three aspects: layout, scale, and vegetation configuration.⁽⁵¹⁾ The scale effect of green space can form urban ventilation corridors, purify the air, and absorb dust. The patch size and shape of natural elements and corridor settings have a direct effect on the purification of air pollutants. The type of green space and vegetation distribution also have a significant effect on regulating the microclimate environment.⁽⁵²⁾ These characteristics are consistent with our findings; therefore, the reasonable arrangement of natural elements can mutually reinforce the mitigation effect on respiratory health risks.

3.4 Policy implications for space environment construction

The identification of the spatial pattern of respiratory health risks and potential risk factors can form the basis for planning and control implementation, making the construction of healthy cities more operable. The key to the optimization of urban spatial environment is to build a low pathogenic spatial exposure environment. According to the main results of this study, the planning and control methods can be carried out in four aspects: (1) Optimization of urban land

use: The focus is on the optimization of the layout of residential, commercial, and public service land to avoid excessive dispersion or concentration; commercial and public service land should form a layout pattern of “small concentration and large dispersion” (commercial and public land of the same level should be appropriately concentrated, whereas commercial and public land of different levels should be dispersed).⁽¹⁵⁾ The balanced layout of residential land can guide the spatial and temporal distributions of population flow, reduce the pressure of traffic flow, and reduce the concentration of a large number of people in high-risk areas. (2) Optimization of urban spatial form: The space form with low floor area ratio, low building density, high ventilation, and high sky openness is beneficial to human respiratory health. Therefore, in urban planning, it is necessary to control the intensity of land development. Because sky openness is the factor that has the strongest effect on respiratory health risk, “high-rise, low-density” development is better than “low-rise, high-density” development. Because the risk is most severe in winter in Shenyang, the optimization and adjustment of urban spatial form have the most significant protective effect on health risk. (3) Optimization of urban road traffic: Urban roads and traffic facilities are a “double-edged sword”, which are both a major source of pollution and an important ventilation corridor in the city; the planning can appropriately increase the density of the road network and the width of the road, and the branch road network can be expanded to avoid the formation of crowded and narrow road forms; at the same time, the high-risk road sections should be protected by applying greening vegetation design. The design of greening barriers on both sides of intersections and roads can be strengthened to build an urban road dust retention network, and the layout of traffic service facilities can be improved to provide a balanced level of service to avoid the excessive concentration of people in traffic facilities and increase the risk of respiratory health exposure. (4) Optimization of urban green space and open space: Green space coverage rate and landscape separation play an important role in the regulation of respiratory health risk; the land area of blue-green space should be increased in the planning and appropriately dispersed layout to maximize the health benefits of green space. More open space should be arranged in high-risk areas to increase the openness of the sky in the area. A network-type green space layout pattern of different levels should be formed in the city construction.⁽⁵³⁾

This study has some limitations. First, we did not combine meteorological environment factors and health risks, primarily because we only had continuous meteorological monitoring data for Shenyang and did not obtain continuous meteorological monitoring data from each monitoring station. Second, the study was based only on the monitoring data of the same horizontal plane in the city, whereas the distribution structure of urban air pollutants and population also presents a vertical distribution trend.⁽⁵⁴⁾ We did not determine the risk pattern of urban vertical space. Therefore, follow-up studies can combine long-term monitoring data of the urban meteorological environment to further verify the key spatial environmental factors affecting respiratory health to form a spatial respiratory health risk pattern in urban longitudinal space.

4. Conclusion

We improved the AQI sensor method and established a respiratory health risk exposure assessment model. The spatial distribution pattern of the respiratory health risks in Shenyang, China, was investigated, and the relationship between spatial environmental factors and respiratory health risk was further analyzed. The results were as follows: the spatial distribution pattern of the health risks in Shenyang in 2019 showed notable spatial heterogeneity and temporal variability. The respiratory health risk was the lowest in autumn and the highest in winter. Overall, 23 types of spatial environmental factor, including land use, spatial form, road traffic, and green space, were highly correlated with respiratory health risks, indicating that they play a role in the formation of such risks. Two of them, urban spatial morphology and green space, were the key factors affecting the degree of respiratory health risk. The geographical detection results showed that the volume ratio, building density, sky openness, ventilation potential coefficient, and landscape shape indicators played a greater role in affecting respiratory health risks than the other spatial environmental factors. The explanatory power of the interaction between any two factors other than the volume ratio factor on respiratory health risks far exceeded that of a single factor. Despite some limitations, the findings provide new perspectives for optimizing the urban spatial environment and designing healthy cities. They stimulate further research on the relationship between urban spatial environments and respiratory diseases, thus contributing to the understanding of urban environmental-respiratory health mechanisms. Finally, we also emphasize the importance of exploring new indicators for assessing the relationship between population and respiratory exposure risk.

Acknowledgments

This work was supported by the National Natural Science Foundation of China (Grant nos. 52378063 and 52308070).

References

- 1 J. Schwartz, K. Fong, and A. Zanobetti: *Environ. Health Perspect.* **126** (2018) 2732. <https://doi.org/10.1289/ehp2732>
- 2 L. Yang, C. Li, and X. Tang: *Front. Cell Dev. Biol.* **8** (2020) 00091. <https://doi.org/10.3389/fcell.2020.00091>
- 3 J. Song, C. Li, M. Liu, Y. Hu, and W. Wu: *Remote Sens.* **14** (2022) 3173. <https://doi.org/10.3390/rs14133173>
- 4 E. A. MacIntyre, U. Gehring, A. Moelter, E. Fuentes, C. Kluemper, U. Kraemer, U. Quass, B. Hoffmann, M. Gascon, B. Brunekreef, G. H. Koppelman, R. Beelen, G. Hoek, M. Birk, J. C. de Jongste, H. A. Smit, J. Cyrus, O. Gruzieva, M. Korek, A. Bergstrom, R. M. Agius, F. de Vocht, A. Simpson, D. Porta, F. Forastiere, C. Badaloni, G. Cesaroni, A. Esplugues, A. Fernandez-Somoano, A. Lerxundi, J. Sunyer, M. Cirach, M. J. Nieuwenhuijsen, G. Pershagen, and J. Heinrich: *Environ. Health Perspect.* **122** (2014) 107. <https://doi.org/10.1289/ehp.1306755>
- 5 Z. Zhen, Y. Yin, H. Zhang, J. Li, J. Hu, L. Li, X. Kuang, K. Chen, H. Wang, Q. Yu, and X. Zhang: *Sci. Total Environ.* **855** (2023) 158975. <https://doi.org/10.1016/j.scitotenv.2022.158975>
- 6 W.-L. Cheng, Y.-S. Chen, J. Zhang, T. J. Lyons, J.-L. Pai, and S.-H. Chang: *Sci. Total Environ.* **382** (2007) 191. <https://doi.org/10.1016/j.scitotenv.2007.04.036>
- 7 A. Goshua, C. Akdis, and K. C. Nadeau: *Allergy* **77** (2022) 1955. <https://doi.org/10.1111/all.15224>
- 8 S. Duangsuwan and P. Jamjareekulgarn: *Sens. Mater.* **32** (2020) 511. <https://doi.org/10.18494/sam.2020.2450>

- 9 X. Li, X. Hu, S. Shi, L. Shen, L. Luan, and Y. Ma: *Chin. Geogr. Sci.* **29** (2019) 917. <https://doi.org/10.1007/s11769-019-1081-8>,
- 10 W. Xu, Y. Tian, Y. Liu, B. Zhao, Y. Liu, and X. Zhang: *Int. J. Environ. Res. Public Health* **16** (2019) 2820. <https://doi.org/10.3390/ijerph16162820>
- 11 Y. X. Huang, B. Guo, H. X. Sun, H. J. Liu, and S. X. Chen: *Atmos. Environ.* **267** (2021) 10. <https://doi.org/10.1016/j.atmosenv.2021.118737>
- 12 S. Sachdeva, R. Kaur, Kimmi, H. Singh, K. Aggarwal, and S. Kharb: *Int. J. Environ. Sci. Technol.* **21** (2023) 18. <https://doi.org/10.1007/s13762-023-05307-8>
- 13 J. Heo, P. J. Adams, and H. O. Gao: *Environ. Int.* **106** (2017) 119. <https://doi.org/10.1016/j.envint.2017.06.006>
- 14 F. Li and T. Zhou: *Cities* **89** (2019) 130. <https://doi.org/10.1016/j.cities.2019.01.025>
- 15 M. Yuan, Y. Song, S. J. Hong, and Y. P. Huang: *Habitat Int.* **69** (2017) 37. <https://doi.org/10.1016/j.habitatint.2017.08.007>
- 16 R. Ewing and R. Cervero: *J. Am. Planning Associ.* **76** (2010) 265. <https://doi.org/10.1080/01944361003766766>
- 17 T. Ge, X. Lv, L. Ma, and X. Shen: *Front. Environ. Sci.* **10** (2022) 910668. <https://doi.org/10.3389/fenvs.2022.910668>
- 18 I. Gryech, M. Ghogho, C. Mahraoui, and A. Kobbane: *Int. J. Environ. Res. Public Health* **19** (2022) 3095. <https://doi.org/10.3390/ijerph19053095>
- 19 Q. Wu and H. Lin: *Sci. Total Environ.* **683** (2019) 808. <https://doi.org/10.1016/j.scitotenv.2019.05.288>
- 20 M. Giardina, P. Buffa, A. M. Abita, and G. Madonia: *Stochastic Environ. Res. Risk Assess.* **33** (2019) 1793. <https://doi.org/10.1007/s00477-019-01723-w>
- 21 C. Katushabe, S. Kumaran, and E. Masabo: *Appl. Syst. Innovation* **4** (2021) 44. <https://doi.org/10.3390/asi4030044>
- 22 G. Onkal-Engin, I. Demir, and H. Hiz: *Atmos. Environ.* **38** (2004) 3809. <https://doi.org/10.1016/j.atmosenv.2004.03.058>
- 23 Y.-C. Lin, S.-J. Lee, C.-S. Ouyang, and C.-H. Wu: *Appl. Soft Comput.* **86** (2020) 105898. <https://doi.org/10.1016/j.asoc.2019.105898>
- 24 W.-M. Song, Y. Liu, J.-Y. Liu, N.-N. Tao, Y.-F. Li, Y. Liu, L.-X. Wang, and H.-C. Li: *Medicine* **98** (2019) e14694. <https://doi.org/10.1097/md.00000000000014694>,
- 25 X. Xue, J. Chen, B. Sun, B. Zhou, and X. Li: *Environ. Sci. Pollut. Res.* **25** (2018) 11468. <https://doi.org/10.1007/s11356-018-1270-5>,
- 26 K. K. Mokoena, C. J. Ethan, Y. Yu, K. Shale, Y. Fan, F. Liu, and J. Rong: *Environ. Sci. Pollut. Res.* **26** (2019) 22512. <https://doi.org/10.1007/s11356-019-05463-w>
- 27 H. Huang, H. Yang, Y. Chen, T. Chen, L. Bai, and Z.-R. Peng: *Urban For. Urban Gree.* **62** (2021) 127154. <https://doi.org/10.1016/j.ufug.2021.127154>
- 28 Y. Xue, J. Chu, Y. Li, and X. Kong: *Toxicol. Lett.* **334** (2020) 14. <https://doi.org/10.1016/j.toxlet.2020.09.007>
- 29 H. Yue and T. Hu: *Int. J. Environ. Res. Public Health* **18** (2021) 6832. <https://doi.org/10.3390/ijerph18136832>
- 30 J. Wei, Z. Q. Li, K. Li, R. R. Dickerson, R. T. Pinker, J. Wang, X. Liu, L. Sun, W. H. Xue, and M. Cribb: *Remote Sens. Environ.* **270** (2022) 17. <https://doi.org/10.1016/j.rse.2021.112775>,
- 31 J. Wei, Z. Q. Li, A. Lyapustin, L. Sun, Y. R. Peng, W. H. Xue, T. N. Su, and M. Cribb: *Remote Sens. Environ.* **252** (2021), 17. <https://doi.org/10.1016/j.rse.2020.112136>
- 32 C. Liu, Y. Hu, Y. Chang, M. Liu, Z. Xiong, T. Chen, and C. Li: *Ecosyst. Health Sustainability* **8** (2022) 2130826. <https://doi.org/10.1080/20964129.2022.2130826>
- 33 H. Huang, X. Zhou, Y. Qu, and H. Zhang: *Dyna*, **97** (2022) 162. <https://doi.org/10.6036/10426>
- 34 M. C. Ekwe, F. Adamu, J. Gana, G. C. Nwafor, R. Usman, J. Nom, O. D. Onu, O. I. Adedeji, S. A. Halilu, and O. M. Aderoju: *Environ. Dev. Sustainability* **23** (2021) 10056. <https://doi.org/10.1007/s10668-020-01046-9>
- 35 P. Hou and S. Wu: *Sci. Rep.* **6** (2016) 23792. <https://doi.org/10.1038/srep23792>
- 36 C. Park, J. Ha, and S. Lee: *Sustainability* **9** (2017) 1338. <https://doi.org/10.3390/su9081338>
- 37 M. J. Nieuwenhuijsen: *Nat. Rev. Cardiol.* **15** (2018) 432. <https://doi.org/10.1038/s41569-018-0003-2>
- 38 L. Zhu, D. Ranasinghe, M. Chamecki, M. J. Brown, and S. E. Paulson: *Atmos. Environ.* **252** (2021) 118267. <https://doi.org/10.1016/j.atmosenv.2021.118267>
- 39 P. M. Mannucci and M. Franchini: *Int. J. Environ. Res. Public Health* **14** (2017) 1048. <https://doi.org/10.3390/ijerph14091048>
- 40 Y. Peng, J. Liu, T. Zhang, and X. Li: *Int. J. Environ. Res. Public Health* **18** (2021) 12160. <https://doi.org/10.3390/ijerph182212160>
- 41 F. Wang, Y. Peng, and C. Jiang: *Sustainability* **9** (2017) 217. <https://doi.org/10.3390/su9020217>
- 42 Z. Huang and X. Du: *J. Urban Plann. Dev.* **144** (2018) 05018017. [https://doi.org/10.1061/\(asce\)up.1943-5444.0000476](https://doi.org/10.1061/(asce)up.1943-5444.0000476)

- 43 F. Wang, M. R. Dong, J. Ren, S. Luo, H. Zhao, and J. Liu: Environ. Dev. and Sustainability **24** (2022) 5531. <https://doi.org/10.1007/s10668-021-01670-z>
- 44 R. M. Harrison, T. Van Vu, H. Jafar, and Z. Shi: Environ. Int. **149** (2021) 106329. <https://doi.org/10.1016/j.envint.2020.106329>
- 45 P. Gao, Y. F. Yang, and L. T. Liang: Appl. Ecology Environ. Res. **18** (2020) 7915. https://doi.org/10.15666/aecer/1806_79157939
- 46 R. Xie, D. Wei, F. Han, Y. Lu, J. Fang, Y. Liu, and J. Wang: Technol. Forecasting Social Change **144** (2019) 421. <https://doi.org/10.1016/j.techfore.2018.04.023>
- 47 S.-J. Mei, J.-T. Hu, D. Liu, F.-Y. Zhao, Y. Li, Y. Wang, and H.-Q. Wang: Energy Build. **155** (2017) 324. <https://doi.org/10.1016/j.enbuild.2017.09.019>
- 48 H. Kim and S. Hong: Land **11** (2022) 23. <https://doi.org/10.3390/land11010023>
- 49 S. Host, E. Chatignoux, C. Leal, and I. Gremy: Revue D Epidemiologie Et De Sante Publique **60** (2012) 321. <https://doi.org/10.1016/j.respe.2012.02.007>
- 50 Y. Jiang, L. Hou, T. Shi, and Q. Gui: Sustainability **9** (2017) 2224. <https://doi.org/10.3390/su9122224>
- 51 E. Coombes, A. P. Jones, and M. Hillsdon: Social Sci. Medi. **70** (2010) 816. <https://doi.org/10.1016/j.socscimed.2009.11.020>
- 52 J. R. Wolch, J. Byrne, and J. P. Newell: Landscape Urban Plann. **125** (2014) 234. <https://doi.org/10.1016/j.landurbplan.2014.01.017>
- 53 C. Zhang, Y. Hu, M. D. Adams, M. Liu, B. Li, T. Shi, and C. Li: Environ. Res. **215** (2022) 114393. <https://doi.org/10.1016/j.envres.2022.114393>
- 54 C. Li, M. Liu, Y. Hu, H. Wang, Z. Xiong, W. Wu, C. Liu, C. Zhang, and Y. Du: Sustainable Cities Soc. **86** (2022) 104144. <https://doi.org/10.1016/j.scs.2022.104144>

About the Authors



Zhenxing Li received his bachelor's degree from Heilongjiang University of Science and Technology in 2013 and his master's degree from Shenyang Jianzhu University in 2017. Since 2019, he has been studying for a doctorate degree in urban and rural planning at Shenyang Jianzhu University. His research interests include urban planning, ecological cities, and healthy cities. (lizhenxing1113@163.com)



Yu Shi received his bachelor's degree from Shenyang Jianzhu University in 2009 and his master's degree from Shenyang Jianzhu University and WISMAR University in Germany in 2012. He received his Ph.D. degree from Tianjin University in 2017. Since 2017, he has been an associate professor at the School of Design and Art of Shenyang Jianzhu University. His research interests include green buildings and healthy cities. (33089573@qq.com)



Peiyong Li received her M.S. degree from Beijing Forestry University, Beijing, in 2014 and her Ph.D. degree from Shenyang Jianzhu University, Shenyang, in 2023. Since 2023, she has been a lecturer at Shenyang Jianzhu University. Her research interests are in low carbon urban planning and green buildings. (lipeiyong@sjzu.edu.cn)



Xiaojuan Xing received her B.S. and M.S. degrees from Beijing Forestry University, Beijing, in 2012 and 2015, respectively. Since 2015, she has been a senior engineer at the Beijing Institute of Surveying and Mapping. Her research interests are urban planning, geographic information, and cartography. (xingxiaojuan@bism.cn)



Jingxue Xie received his master's degree in March 2023 from Tokyo University of Agriculture and Technology (TUAT), Tokyo, Japan. He entered the Ph.D. program at TUAT in April 2023 and received Fellow status from the Japan Science and Technology Agency SPRING-FLOuRISH Fellowship for Support for Pioneering Research Initiated by the Next Generation. His main research interests are in urban geography, street perception, and urban environment. (leotse07@gmail.com)



Tiemao Shi received his bachelor's degree from Shenyang Institute of Civil Engineering and Architecture in 1982 and studied in the Department of Architecture, Nanjing Institute of Technology from 1982 to 1984. In 2000, he received his Ph.D. degree from Shenyang Institute of Applied Ecology, Chinese Academy of Sciences. Since 1998, he has been a professor at the School of Architecture and Planning, Shenyang Jianzhu University. His research interests include ecological urbanization, low-carbon cities, and healthy cities. (tiemaos@sjzu.edu.cn)



Yaqi Chu received her bachelor's degree from Shenyang University of Technology in 2009 and her master's degree from Shenyang Architecture University and WISMAR University, Germany, in 2012. She received her PhD degree from Tianjin University in 2020. She has been a lecturer of architecture in Shenyang University since 2020. Her research interests include eco-city and green building. (417185790@qq.com)

